Neutron Detection via the Cherenkov Effect

Z. W. Bell, *Member, IEEE,* L. A. Boatner

***Abstract*-- We have incorporated neutron-absorbing elements in transparent, non-scintillating glasses and used the Cherenkov effect to convert neutron-induced beta-gamma radiation directly into light. Use of the Cherenkov effect requires glasses with a high index of refraction (to lower the threshold and increase the number of Cherenkov photons), and neutron absorbers resulting in radioactive products emitting high-energy beta or gamma radiation. In this paper, we present a brief description of the requirements for developing efficient Cherenkov-based neutron detectors, show the results of measurements of the response of representative samples to a thermal neutron flux, and give the results of a calculation of the expected response of a detector to a moderated fission spectrum.**

I. Introduction

Among the techniques employed in neutron dosimetry and spectrum reconstruction are measurements with activation foils [1]. This technique is particularly well suited to dose and spectrum reconstruction subsequent to a criticality accident because the intense radiation pulse or pulses accompanying accidents do not blind or disable foils. Rather, they record an "image" of the event in the induced radioactivity. In contrast to this, the photosensor in a scintillator-based instrument will likely be blinded by the light and will not recover until the event has ended.

In the usual practice, after exposure to an unknown neutron flux, the alpha, beta, or gamma radiation from the activated material are measured in a known geometry with a calibrated detector to obtain the total number of radioactive atoms produced. Using the cross sections for production of the radioactive species and the physical characteristics of the foil, the spectrum-integrated response can deduced, and an estimate of the incident spectrum is obtained from measurements of a number of exposed foils. However, this practice requires that the activation foil be retrieved, and this may lead to unwanted exposure of personnel to the radioactive environment caused by the criticality.

The radiation emitted by the activation product determines the geometry of the target that minimizes the effects of self-absorption of the incident neutron flux and the self-absorption of outgoing radiation to be detected. For alpha counting, foils must be only a few microns thick (the range of a 5.5 MeV alpha is only 25 microns in aluminum, for example), while for beta counting, the foils should be under 100 microns (the range of a 1 MeV beta is approximately 1 mm in aluminum). Therefore, particle-counting foils must either contain isotopes with large cross sections or the foils must have large areas (so that sufficient absorber can be exposed to the flux), or both. These effects require the application of self-absorption corrections that can significantly affect the precision of the measurement. However, this problem can be eliminated if the activation product is intimately integrated into a detecting system. In such a system, the characteristic radiation will be completely absorbed in the scintillator and no self-absorption correction would be required regardless of the size of the neutron absorber.

Exploitation of the Cherenkov effect [2],[3] offers a possible solution to the problems of retrieval, blinding, and self-absorption because many isotopes used in activation foils emit high-energy beta particles and/or gamma rays. By mixing the neutron-sensitive species into a clear, non-scintillating medium (such as glass) Cherenkov light will be generated as the induced radioactivity decays. Decomposition of the decay of the intensity of the Cherenkov light into a sum of decreasing exponentials identifies each radioactive species present and provides the information needed to determine the total activation of the neutron absorber, while the intimate mixture of the absorber with the Cherenkov medium guarantees complete absorption of the beta particles. Then, since counting of the activated absorber can commence *after* the event, by keeping the photosensor off until a criticality event is detected by a different detector, blinding of the photosensor is avoided. Consequently, an instrument based on the Cherenkov effect need consist of only the absorbing medium, a photosensor, a threshold detector, a multichannel scaler and a wire or radio to transmit the data to a remote location.

The major drawback of using the Cherenkov effect is that only 100 – 300 photons/MeV are produced. However, since spectroscopy is not necessary (recall that it is only necessary to count Cherenkov photons), even this objection is overcome.

Manuscript received November 16, 2007. This work was supported by the U.S. Department of Energy, Office of Research and Engineering (NA-22). Oak Ridge National Laboratory is managed for the U. S. Department of Energy under contract DE-AC05-00OR22725.

Z. W. Bell is with the Oak Ridge National Laboratory, Oak Ridge, TN 37831 USA (telephone: 865-574-6120, e-mail: bellzw@ornl.gov).

L. A. Boatner is with the Oak Ridge National Laboratory, Oak Ridge, TN 37831 USA (telephone 865-574-5492).

II. Cherenkov Considerations

The emission of Cherenkov light is a consequence solely of the index of refraction of the medium and the speed of the charged particle traversing it [4]. For energies under a few hundred MeV, only electrons and positrons can produce Cherenkov light. Because there is a threshold for the emission of Cherenkov light by electrons, non-scintillating media will not respond to low-energy gamma radiation (which produces Compton electrons and photoelectrons) or to electrons with energies below ~100 keV. However, every electron with energy above the Cherenkov threshold will produce photons and thus provide a real-time signature from which the activation level can be deduced.

Fig. 1 shows the threshold for the production of Cherenkov light by both photons and electrons. The index of refraction of Pb-In-phosphate glass (one of the materials tested for this work) is indicated.

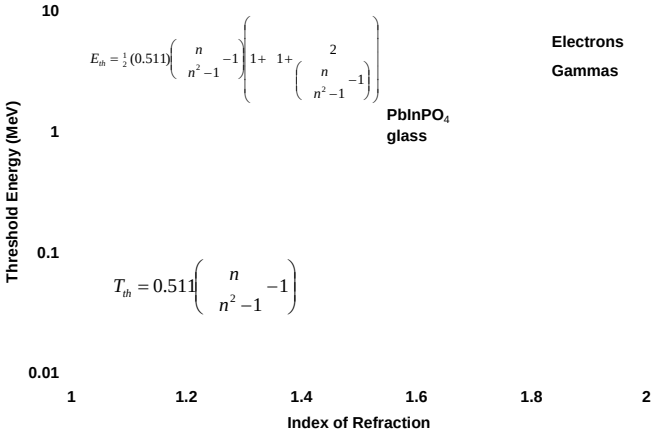

Fig. 1. Cherenkov thresholds.

The curve for gamma rays is a calculation of the minimum energy gamma ray that can produce a Compton electron sufficiently energetic to produce Cherenkov light. That is, the most energetic Compton electron that can be produced by a 220 keV gamma ray is ~100 keV. Consequently, in a glass whose index of refraction is 1.8, gamma rays with energy lower than 220 keV cannot produce Cherenkov light. The threshold for gamma rays to produced photoelectrons with energy greater than 100 keV is simply E_γ+E_b, where E_b is the electron binding energy.

The existence of thresholds implies that it is necessary to choose activation materials carefully. It is necessary that the activation product decay with the emission of energetic betas and/or gammas. Some candidate reactions are shown in Table I, below. The list is not meant to be exhaustive, but does include elements that are constituents of glass.

All of these reactions produce high-energy beta particles and/or gamma rays. Some are most sensitive to thermal neutrons; aluminum can be sensitive to both thermal and fast neutrons. In all cases, however, the half-lives of the reaction products are short (ranging from only 134 s to 2.6 h), placing these isotopes among those useful for rapid dose and spectrum reconstruction.

Table I
Some Candidate Absorbers and Reactions

Reaction	Cross Section (barns)
$^{115}In(n,\gamma)^{116}In^*$	194[a]
$^{27}Al(n,\gamma)^{28}Al$	0.23[a]
$^{164}Dy(n,\gamma)^{165}Dy$	2700[a,b]
$^{56}Fe(n,p)^{56}Mn$	0.1[c]
$^{28}Si(n,p)^{28}Al$	0.1 – 0.4[d]
$^{27}Al(n,\alpha)^{24}Na$	0.13[c]

[a] Thermal neutrons
[b] Includes ground state and first excited state production
[c] Maximum value in energy range from threshold to 14 MeV
[d] Over energy range from threshold to 14 MeV

III. Measurements

Activations were performed with a moderated AmLi source producing approximately 100 n/cm^2/s. Consequently, thermal neutron absorbers were realized by fabricating $PbInPO_4$ (30 g $PbHPO_4$ + 3.5 g In_2O_3) and $CaNaPO_4$:$DyCl_3$ (16%) glass. The $PbInPO_4$ sample was cylinders 2.54 cm in diameter and 1.2 cm thick; the Dy glass had the same diameter, but was only 4 mm thick. One face was polished flat for coupling to a photomultiplier. The $PbInPO_4$ sample is shown in Fig. 2.

Fig. 2. $PbInPO_4$ Glass sample.

The glasses were prepared by melting the raw materials together, allowing the molten mixture to cool slightly, pouring the liquid into a BN boat, and annealing overnight. The $PbInPO_4$ was not observed to be fluorescent under UV light, while the Dy glass exhibited yellow fluorescence under 366 nm UV, but not under 254 nm light. Counting was performed by coupling the glass samples to a Photonis XP2020Q photomultiplier operated at -2000 V and whose anode was monitored by an ORTEC 584 discriminator operated in leading edge mode (timing is not needed for these measurements) with the threshold set at 50 mV. The TTL output of the discriminator drove a Tukan 8K USB [5] operating in MCS (multichannel scaler) mode. The Tukan acquired counts in 8192 time bins with widths of 1 second (In), or 2 seconds (Dy).

Fig. 3 shows the decay of the $PbInPO_4$ glass. Three components were required to fit the data: 2.6- and 54-minute

half-lives and a constant 10 count/sec "background." The 2.6-minute half-life was initially attributed to the recovery of the photomultiplier from exposure to ambient lighting during mounting of the glass sample.

The 54-minute half-life corresponds to the In decay. Accounting for the 10 minutes required to transport and mount the activated sample, the initial count rate was estimated to be 130 counts/second. MCNP5 [6] calculations of the absorption of neutrons incident on the flat face predicted that 53% would be captured by In, while 57% of thermal neutrons incident on the curved surface should be captured. Given the dimensions of the samples and the flux from the source, a total rate of 992 n/s was expected, leading to an estimated efficiency of 13%. Of course, this value depends on the threshold and light collection and could be improved or worsened depending on operating conditions.

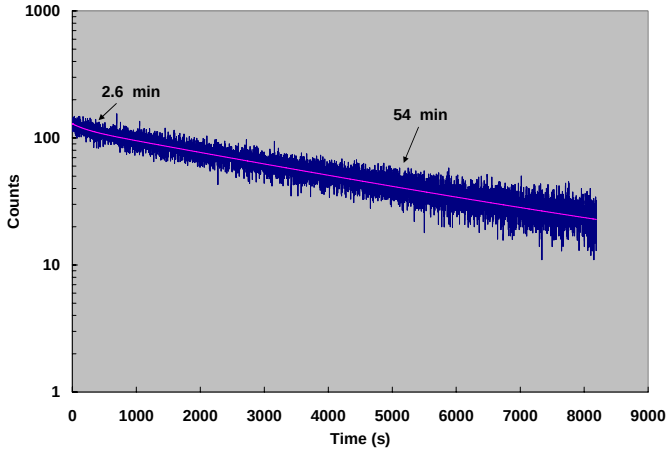

Fig. 3. Decay of activity of $PbInPO_4$ glass. The MCS used 1-second bins.

Because In produces beta particles with endpoint energies between 600 keV and 1.01 MeV, and gamma rays with energies 1294 (84%), 1097 (56%), 416 (29%), 2112 (16%), 819 (12%), and 1508 keV (10%), it was necessary to demonstrate that the events generated by the photomultiplier were, in fact, from light rather than from decay radiations interacting directly with the photomultiplier. Such interactions occur in the photocathode itself, the photomultiplier's window, and the dynode structure. Therefore, a 25 μm (0.001 inch) aluminum foil was placed over the photomultiplier window to block the light (but not the betas and gammas) and the In experiment was repeated. The results are shown in Fig. 4.

The "Foil over" data were obtained with only the foil covering the photomultiplier window; a fairly constant 10 counts/s are observed. The "Glass over foil over" data were obtained when the activated glass was placed over the foil. A few counts/s are observed indicating that direct beta/gamma interactions are no more than a few per cent of the total. This is qualitatively consistent with calculations of the range of ^{116m}In's beta particles and the distribution of neutron absorption over the volume of the glass.

Similar experiments were performed with the Dy glass, with the results shown in Fig. 5. The data was fit with three decaying exponentials, with one of the half-lives fixed at 54 minutes, plus a constant. The amplitude of the 54-minute component was always driven to zero, while one component was driven to 140 minutes (the half-life of ^{165}Dy) and the other component was driven to 9.2 minutes. The constant background count rate was 20 counts/s.

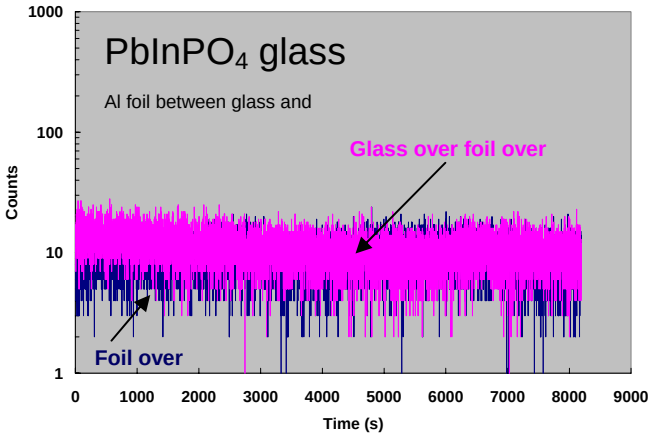

Fig. 4. Demonstration that observed decay is due to light. The MCS used 1-second bins.

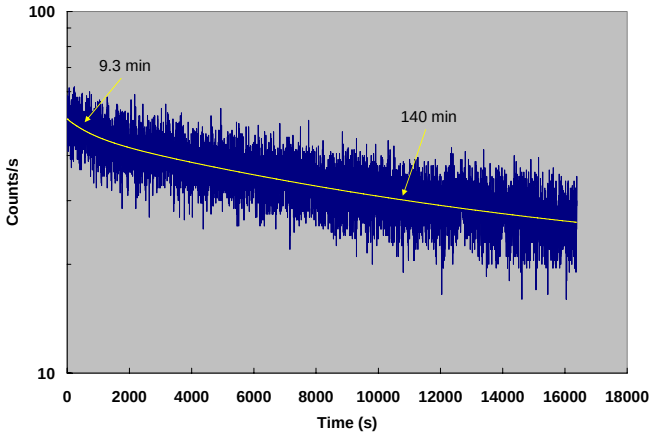

Fig. 5. Decay of activity of $CaNaPO_4$:$DyCl_3$ glass. The MCS used 2-second bins because of the half life of ^{165}Dy.

The amplitude of the Dy exponential was only 13 counts/s, in stark contrast to the 130 counts/s In data and despite the much larger capture cross section of ^{164}Dy. Simply using the published thermal capture cross sections of Dy and In the ratio of Dy and In initial count rates is expected to be approximately 1.1. Part of this discrepancy can be explained by the differences in the decay modes and the effect of the fixed threshold. Note that ^{165}Dy emits two beta particles with average energies of 454 (83%) and 415 (15%) keV, while emitting essentially no gamma rays capable of producing Cherenkov light [7]. Indium, on the other hand, while producing beta particles with somewhat lower average energies of 352 (52%), 295 (34%), and 190 keV (10%), and hence less Cherenkov light, produces approximately 2 gamma rays per decay capable of producing energetic Compton electrons and photoelectrons. The gamma energies and

absolute emission probabilities per decay have been listed above; the average energy is in excess of 1 MeV. The Compton electrons and photoelectrons serve to increase the amplitude of the Cherenkov signal because they are emitted essentially simultaneously with the beta decay and the counting electronics cannot distinguish them temporally from the beta particles. MCNP5 calculation of the number of Compton electrons and photoelectrons in $PbInPO_4$ indicates that approximately 1.5 photon-produced electrons per decay should be expected. Consequently, it seems likely that the 50 mV threshold, while suitable for light from the In decays, should have been lowered for the Dy measurement.

The factor of 10 between the expected and measured ratio is, however, too great to be explained solely by the differences in decay modes. The index of refraction of the $CaNaPO_4$ glass varies between 1.55 (400 nm) and 1.52 (800 nm) [8] leading to a Cherenkov threshold of 164 keV for electrons (as opposed to the 104 keV in $PbInPO_4$), and causing a faster extinction of the Cherenkov light. Lastly, it remains necessary to measure the absorption of light as a function of wavelength to rule out the possibility that the $CaNaPO_4$ glass is simply more absorptive at shorter wavelengths. The fact that this glass was observed to exhibit yellow fluorescence when exposed to 366 nm ultraviolet light may mean that Cherenkov light fluoresces the Dy ions thereby shifting the emission to wavelengths at which the photomultiplier is not as sensitive. Again, this implies that the 50 mV threshold was somewhat suboptimal.

A comparison of the initial decaying components in Figs. 3 and 5 shows that different half-lives were observed. While it was initially thought that the 2.6 minute component in Fig. 3 was caused by exposure of the photomultiplier to ambient lights, the observation of a 9.3 minute component may cast doubt on that attribution. The same photomultiplier was used in both measurements and the samples were mounted in the same laboratory, which tends to discount the theory of the same source as the cause of the fast component. A possible explanation for the different half-lives is that there are different and as yet unknown impurities in the two glass samples. Additional experiments with a bare photomultiplier are required to isolate decay components related to exposure to ambient light.

It is important to understand the sensitivity of the estimate of half-life to initial count rate because the confirmation of the radioactive species responsible for Cherenkov light depends on this. In the case of a single half-life, with data recorded by an MCS with bin time much less than the half-life (as was the case here), the counts, N_i, in the bin starting at time t_i are given by

$$N_i = A\delta e^{-t_i/\tau} \tag{1}$$

where δ is the MCS bin width, A is the initial count rate, and τ is $t_{1/2}/\ln(2)$, the inverse of the decay constant. τ can be computed from measurements at times t_1 and t_2:

$$\tau = \frac{t_2 - t_1}{\ln\left(\frac{N_1}{N_2}\right)} \tag{2}$$

If it is assumed that there are no statistical correlations between the two measurements, then the relative uncertainty in τ is given by

$$\frac{\Delta\tau}{\tau} = \sqrt{\frac{1+\frac{N_1}{N_2}}{N_1\left(\ln\left(\frac{N_1}{N_2}\right)\right)^2}} \tag{3}$$

If N_2 is measured approximately one half-life after N_1 (as can be inferred from the measurements described above), then (3) reduces to

$$\frac{\Delta\tau}{\tau} = \sqrt{\frac{3}{N_1(\ln(2))^2}} = \frac{2.5}{\sqrt{N_1}} \tag{4}$$

For N_1 = 100, the half-life can be determined with 25% precision, while when only 10 counts are in the initial bins, the uncertainty in the half-life can approach 80%. Manual adjustment of the computed half-life of the Dy from the data in Fig. 5, indicated that although a value of 140 minutes is optimal, values as large as 180 minutes could not be absolutely ruled out. Clearly, in this particular Dy glass, a more intense neutron source would have produced better data.

IV. Monte Carlo Simulations

We used MCNP5 to estimate the response to a criticality of $PbInPO_4$ glass shielded by 1 meter of concrete. The fission spectrum was simulated by a Watt distribution with parameters appropriate for ^{235}U and the concrete was modeled as "Los Alamos" concrete containing 8.5% hydrogen, 60% oxygen, 2.5% aluminum, 24% silicon, 2% calcium, and trace amounts of sodium, magnesium, potassium, and iron. The resulting spectrum and In capture cross section are shown in Fig. 6, from 0.01 eV to 10 MeV.

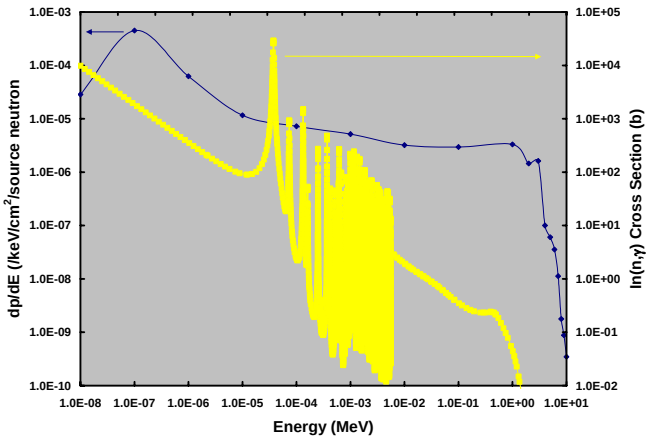

Fig. 6. Calculated fission spectrum moderated by 100 cm of concrete plotted together with the In(n,γ) cross section.

The spectrum is expressed as probability per unit energy per cm^2 per source neutron) and uses the left axis. The spectrum exhibits a thermalized (but not thermal) peak near 0.1 eV. The spectrum is not insignificantly small up to 1 MeV. Consequently, resonance capture is expected to contribute to the induced radioactivity. The In capture cross section (the yellow data set) uses the right axis. MCNP5 predicted that 2.75% of the source neutrons reached the surface of a concrete sphere; the remainder was captured within the concrete. Simulation of the spectrum in Fig. 6 impinging onto a 5.08 cm diameter by 1 cm thick cylinder of glass indicated that 46.7% of the incident neutrons would be captured by indium.

These data can be used to estimate the response of the $PbInPO_4$ glass to a criticality. The number of captures per gram of fissioned ^{235}U is given approximately by

$$N = \frac{0.0275 \times 0.467 \times 3 \times 6.022 \times 10^{23}}{4\pi \times 10^4 \times 235}$$

$$= 7.86 \times 10^{14} / g / cm^2$$

Three neutrons per fission were assumed here; the first two factors in the denominator convert the probability per source neutron to a flux. For an accident in which even 1 μg of ^{235}U fissions, the initial induced activity would be expected to be 786 MBq from a 1 cm^2 area piece of glass 1 cm thick. Using the observed efficiency of 13% leads to a count rate from a photomultiplier of approximately 10^8 counts/s. Clearly, the calculation suggests that $PbInPO_4$ should be quite sensitive to a criticality and this sensitivity is confirmed by the response to the 100 n/cm^2/s AmLi source used in the measurements described above.

V. CONCLUSIONS

The information presented above demonstrates that the Cherenkov effect can be used for the detection of neutrons through the measurement of induced radioactivity. This technique has the advantages that the detecting medium need not contain any scintillator (making the formulation simpler, and making it insensitive to external beta radiation), is extremely fast (Cherenkov light is produced on a time scale shorter than 1 ns), and it eliminates the need for self-absorption corrections because the essentially all the particles responsible for Cherenkov light are stopped within the converter.

A detector based on Cherenkov light is simply a pulse counting instrument requiring no spectroscopy electronics. That is, only a Cherenkov converter, photosensor, power supply, discriminator, and a multichannel scaler are needed. Pre-deployment of such an instrument, with appropriate communications channels, eliminates the need to retrieve the detecting medium for off-site/off-line counting. This enables the use of isotopes having half-lives of minutes to hours instead of hours to days, and permits dose reconstruction to be completed rapidly.

The use of glass detectors offers advantages of potential mass production, the ability to incorporate many materials used in activation foils, and robust physical characteristics making the material likely to survive a criticality event at a reactor. However, any optically clear medium with low attenuation at short wavelengths can be used. The medium should not be fluorescent at Cherenkov wavelengths since this will tend to shift the emission away from the region of maximum sensitivity of a photocathode. If, however, a solid-state photosensor is used, this requirement may be relaxed.

The main disadvantage of this technique is that the amount of light produced by relatively low-energy electrons is only about 1% that produced by scintillators. Consequently, quiet or perhaps cooled photosensors must be used. In addition, when a photomultiplier is used, a quartz window is required.

VI. REFERENCES

[1] Glenn F. Knoll, *Radiation Detection and Measurement*, 3rd Edition. New York: John Wiley and Sons, 2000, p. 485.

[2] P. A. Cherenkov, *Dokl. Akad. Nauk SSSR* **2**, 451 (1934).

[3] S. I. Vavilov, *Dokl. Akad. Nauk SSSR* **2**, 457 (1934).

[4] J. D. Jackson, *Classical Electrodynamics*, pp. 494 – 499, John Wiley & Sons, 1962.

[5] Manufactured by the Andrzej Soltan Institute for Nuclear Studies, Department of Detectors and Nuclear Electronics, 05-400 Otwock-Swierk, Poland.

[6] X-5 Monte Carlo Team, *MCNP-A General Monte Carlo N-Particle Transport Code, Version 5*, LA-UR-03-1987 (Revised 10/3/2005), available from the Radiation Safety Information Computational Center, Oak Ridge National Laboratory, www-rsicc.ornl.gov.

[7] National Nuclear Data Center, Interactive Chart of the Nuclides, available at www.nndc.bnl.gov.

[8] S. W. Allison, L. A. Boatner, B. C. Sales, US Patent 5,812,729, issued September 22, 1998.